A class of Bessel function integrals with application in particle physics

1993 J. Phys. A: Math. Gen. 26 7547

(http://iopscience.iop.org/0305-4470/26/24/027)

J. Phys. A: Math. Gen. 26 (1993) 7547–7562. Printed in the UK

A class of Bessel function integrals with application in particle physics

I P Grant and H M Quiney†
Mathematical Institute, University of Oxford, 24–29 St Giles', Oxford, OX1 3LB, UK

Received 18 May 1993

Abstract. Many problems in particle physics and field theory require the evaluation of integrals of the form

$$I_{l_1,l_2,l_3}(p_1, p_2, p_3) = \frac{4p_1p_2p_3}{\pi}\int_0^\infty r^2 j_{l_1}(p_1r)j_{l_2}(p_2r)j_{l_3}(p_3r)\,\mathrm{d}r.$$

Our investigation arose in connection with a new method of partial wave mass renormalization of the electron self-energy in quantum electrodynamics (QED) where these integrals play a crucial role. Previous studies appear not to have led to expressions which are readily computable. We derive an explicit formula for the general case and a recursive method of construction which allows us to generate all cases of practical interest to high precision. Our algorithms are highly efficient on scalar computers and readily vectorize on suitable machines.

1. Introduction

This paper concerns the calculation of the integrals

$$I_{l_1,l_2,l_3}(p_1, p_2, p_3) = \frac{4p_1p_2p_3}{\pi}\int_0^\infty r^2 j_{l_1}(p_1r)j_{l_2}(p_2r)j_{l_3}(p_3r)\,\mathrm{d}r \tag{1}$$

involving the product of three spherical Bessel functions of real, positive argument. For non-negative integer l, the spherical Bessel functions are related to the Bessel functions whose order is half an odd integer by

$$j_l(z) = \left(\frac{\pi}{2z}\right)^{1/2} J_{l+1/2}(z).$$

The integrals in (1) can be expressed in terms of the integrals

$$\int_0^\infty J_{l_1+1/2}(az)J_{l_2+1/2}(bz)J_{l_3+1/2}(cz)z^{1/2}\,\mathrm{d}z. \tag{2}$$

These integrals are related to the discontinuous integrals of Weber and Schafheitlin [1–3]. The special case of (1) in which $l_1 = 0$ and $l_2 = l_3$ can be related to formula (6.578.8) of [3]. In the present notation this reads

$$I_{0,l,l}(p_1, p_2, p_3) = \frac{4p_1p_2p_3}{\pi}\int_0^\infty r^2 j_0(p_1r)j_l(p_2r)j_l(p_3r)\,\mathrm{d}r = P_l(\cos\theta_1) \tag{3}$$

† Now at Clarendon Laboratory, University of Oxford, Parks Road, Oxford, OX1 3PU, UK.

0305-4470/93/247547+16$07.50

where θ_1 is real-valued and is given by

$$\cos\theta_1 = (p_2^2 + p_3^2 - p_1^2)/(2p_2p_3)$$

for values of p_1, p_2 and p_3 for which this makes sense. The derivation of the formula on which (3) is based is given by Watson ([1], pp 411–2). Related work is described by Bailey [4], and Gervois and Navelet [5] have discussed similar integrals which have applications to phenomenological calculations in high-energy physics using the Regge formalism. An explicit formula for (1) was given by Jackson and Maximon [7] which was later employed by Danos *et al* [8] in treating a problem in dtμ muon-catalysed fusion. The Jackson–Maximon formula is equivalent to our (18) below, as is the result of Davies and Davies [9] which was applied by Davies *et al* [10] to the calculation of Green's functions in pion–nucleon scattering†.

The 'vertex integrals' (1) appear in the calculation of radiative transition amplitudes for free electrons. We encountered them in devising a new method of renormalization of the self-energy of a bound electron; a brief outline of the scheme is given in [11]. Textbooks quote from the early papers of Feynman [12, 13] and others (see, for example, the review by Mohr in [14]) which lead to an expansion of the self-energy of a bound electron in a hydrogenic atom in powers of $Z\alpha$ and $Z\alpha$ ln $Z\alpha$. It was realized quite early, for example by Brown *et al* [15], that this series is very slowly convergent — indeed it is not known for certain whether it is truly convergent — and non-perturbative methods are therefore preferred, particularly for higher values of Z. The first non-perturbative calculation was proposed by Brown *et al* [15] and carried out by Brown and Mayers [16], later corrected by Desiderio and Johnson [17]. Mohr [18, 19] used a somewhat different approach for calculations of the self-energy of $n = 1, 2$ states which form the basis of the extensive tables of radiative corrections to electron binding energies in hydrogenic atoms by Johnson and Soff [20]. Mohr and Kim [21] used similar methods for hydrogenic $n = 3, 4$ states. Cheng and Johnson [22] and others extended the method of [15] to deal with finite nuclear size effects, and Cheng *et al* [23] have recently made such calculations for $n = 2, 3, 4$ states. Snyderman [24] suggested a major technical improvement which has been implemented in [25]. Further extensions to compute the self-energy of electrons in atomic mean-field potentials were reported at the *Nobel Symposium No. 85 on Heavy Ion Spectroscopy and* QED *Effects in Atomic Systems* in 1992 and are in course of publication in the journal *Physica Scripta* and elsewhere.

These renormalization procedures, though well established, involves both theoretical and numerical difficulties. The self-energy calculation can be regarded as a perturbation correction to the binding energy arising from processes in which the electron jumps to a virtual excited state through an interaction with the quantized radiation field before returning to its initial state. The total self-energy from all such virtual processes is infinite for both free and bound electrons, and it is usual to argue that the free self-energy is already taken into account in the observed electron mass. The correction to the binding energy of an atomic state therefore comes from the difference of two related calculations: one in which the electron propagates in the virtual states of the atomic field and one in which the virtual states are those of a free electron. Feynman [12, 13] gave a simple operator form for the self-energy of a free electron wave packet, and the conventional method of renormalization identifies the relevant terms analytically and discards them so that only the finite remainder is calculated. This is still a formidable numerical calculation, involving both high-frequency photons and large angular momenta, and numerical convergence is slow. The strategy of

† The reader should note that Davies *et al* [10] use a notation similar to (1) but without the normalizing factor $4p_1p_2p_3/\pi$.

[11] aims to exploit the fact that the contribution of different radiation multipoles to the self-energy is additive; individual multipoles give finite contributions (though their sum is infinite without renormalization) and we have found that the sum of renormalized multipole contributions converges more rapidly to a finite result.

The next section contains a brief survey of elementary properties of the integrals (1) and of the special functions appearing in the analysis. An elementary application of the Cauchy residue theorem is used to derive an explicit algebraic formula in section 2.3; this is rather similar to a formula of Gervois and Navelet [6] who used a rather different method of derivation. It is, however, totally unsuitable for the target application, and this has led us to develop the novel recursive algorithms reported in section 3. They have excellent numerical stability and can be programmed very efficiently on both serial and vector processors. We give in section 4 a simple illustration of the way in which the vertex integrals can be used in quantum mechanics and in the construction of the multipole counter terms in [11] and comment on the advantages of our method in comparison with alternative methods of calculation in section 5.

2. An explicit formula

2.1. Elementary properties of the integrals

Inspection of equation (1) reveals that the integrals $I_{l_1,l_2,l_3}(p_1, p_2, p_3)$ are invariant with respect to a simultaneous permutation of the subscripts of both the order parameters l_1, l_2, l_3 and the momentum parameters p_1, p_2, p_3 by the same permutation

$$P = \begin{pmatrix} 1 & 2 & 3 \\ i & j & k \end{pmatrix}$$

so that

$$I_{l_1,l_2,l_3}(p_1, p_2, p_3) = I_{l_i,l_j,l_k}(p_i, p_j, p_k) \tag{4}$$

for all such permutations.

It is also easy to see that $I_{l_1,l_2,l_3}(p_1, p_2, p_3)$ only depends on the *ratios* of the momenta, that is for any number $\alpha > 0$,

$$I_{l_1,l_2,l_3}(p_1, p_2, p_3) = I_{l_1,l_2,l_3}(\alpha p_1, \alpha p_2, \alpha p_3). \tag{5}$$

We shall see later that each vertex must conserve 3-momentum, so that the magnitudes p_1, p_2, p_3 must be able to form the sides of a plane triangle. Thus every non-zero vertex integral contains the function

$$\Delta(p_1, p_2, p_3) := \begin{cases} 1 & \text{if } (p_1, p_2, p_3) \text{ form a non-degenerate triangle} \\ \frac{1}{2} & \text{if } (p_1, p_2, p_3) \text{ form a degenerate triangle} \\ 0 & \text{otherwise.} \end{cases} \tag{6}$$

as a factor. It follows from (5) that $I_{l_1,l_2,l_3}(p_1, p_2, p_3)$ can be expressed entirely in terms of the angles $\theta_1, \theta_2, \theta_3$ of the triangle opposite to the sides p_1, p_2, p_3, respectively. Indeed since the sides of such a triangle satisfy the sine rule,

$$(\sin\theta_1)/p_1 = (\sin\theta_2)/p_2 = (\sin\theta_3)/p_3$$

we can immediately replace $p_i, i = 1, 2, 3$, by the corresponding value $\sin\theta_i$ without any scaling factor. The freedom to make this replacement, an important consequence of the normalization factor introduced in (1), will be put to good use later.

The discontinuous character of the integrals $I_{l_1,l_2,l_3}(p_1, p_2, p_3)$ can be exhibited by elementary methods in the simplest case in which $l_1 = l_2 = l_3 = 0$ when we note that

$$j_0(z) = (\sin z)/z$$

and that for any real number a

$$\int_{-\infty}^{\infty} \frac{\sin az}{z}\,\mathrm{d}z = \pi \operatorname{sgn} a.$$

The integrand and the integral are both identically zero when a is zero. We see that

$$I_{0,0,0}(p_1, p_2, p_3) = \frac{4}{\pi}\int_0^{\infty} \sin(p_1 r)\sin(p_2 r)\sin(p_3 r)\frac{\mathrm{d}r}{r}.$$

Since

$$\sin x \sin y \sin z = \tfrac{1}{4}\{\sin(x + y - z) + \sin(y + z - x) + \sin(z + x - y) - \sin(x + y + z)\}$$

and the numbers p_i are by definition non-negative, we see that

$$I_{0,0,0}(p_1, p_2, p_3) = \tfrac{1}{2}\{\operatorname{sgn}(p_1 + p_2 - p_3) + \operatorname{sgn}(p_2 + p_3 - p_1) + \operatorname{sgn}(p_3 + p_1 - p_2) - 1\}$$

where $\operatorname{sgn}(x)$ denotes the sign of x. When the three momenta p_1, p_2, p_3 can be the sides of a non-degenerate plane triangle, all the expressions $\operatorname{sgn}(p_i + p_j - p_k)$ have the value $+1$ and the right-hand side sums to unity; if, say, the side p_3 is longer than the sum of the other two sides, then $\operatorname{sgn}(p_1 + p_2 - p_3) = -1$, and the right-hand side sums to zero. In the degenerate case, $p_3 = p_1 + p_2$, and the first term is zero. We therefore have

$$I_{0,0,0}(p_1, p_2, p_3) = \Delta(p_1, p_2, p_3) \tag{7}$$

This is, of course, in agreement with the more general result of (3).

2.2. *Properties of spherical Bessel functions*

The properties of spherical Bessel functions of the first kind, related to the ordinary Bessel functions by

$$j_l(z) = \left(\frac{\pi}{2z}\right)^{1/2} J_{l+1/2}(z) \tag{8}$$

are crucial to our analysis. They are the solutions, bounded at the origin, of the second-order differential equation

$$z^2\frac{\mathrm{d}^2 w}{\mathrm{d}z^2} + 2z\frac{\mathrm{d}w}{\mathrm{d}z} + [z^2 - l(l+1)]w = 0. \tag{9}$$

The power series expansion is

$$j_l(z) = (2z)^l \sum_{k=0}^{\infty} \frac{(l+k)!}{(2l+2k+1)!}\frac{(-z^2)^k}{k!} \tag{10}$$

where $l = 0, 1, 2, \ldots$. This power series expansion converges for all finite $z \in C$.

The spherical Bessel function can also be expressed in terms of the spherical Hankel functions, defined by the formulae

$$h_l^{(1)}(z) = \mathrm{i}^{-l}\frac{\mathrm{e}^{\mathrm{i}z}}{\mathrm{i}z}\sum_{k=0}^{l}(l+\tfrac{1}{2},k)(-2\mathrm{i}z)^{-k} \tag{11}$$

$$h_l^{(2)}(z) = \mathrm{i}^{l}\frac{\mathrm{e}^{-\mathrm{i}z}}{-\mathrm{i}z}\sum_{k=0}^{l}(l+\tfrac{1}{2},k)(2\mathrm{i}z)^{-k} \tag{12}$$

where $(l+\frac{1}{2},k) = (l+k)!/k!(l-k)!$. Then

$$j_l(z) = \tfrac{1}{2}[h_l^{(1)}(z) + h_l^{(2)}(z)]. \tag{13}$$

It follows that $h_l^{(1)}(z)$, $h_l^{(2)}(z)$ are meromorphic functions of z in any bounded region $\mathcal{G} \subset C$ having poles of order $l+1$ at $z=0$. We also see that $h_l^{(1)}(z)$ tends to zero as $\operatorname{Im} z \to +\infty$ and is unbounded in the lower half of the z-plane. Similarly $h_l^{(2)}(z)$ tends to zero as $\operatorname{Im} z \to -\infty$ and is unbounded in the upper half of the z-plane. The relations

$$f_l(-z) = (-1)^l f_l(z) \tag{14}$$

where $f_l(z)$ can be any of $j_l(z)$, $h_l^{(1)}(z)$ or $h_l^{(2)}(z)$ and

$$\overline{h_l^{(1)}(z)} = h_l^{(2)}(\overline{z}) \tag{15}$$

will also be useful. Finally, we shall require the recurrence relation

$$j_{l+1}(z) + j_{l-1}(z) = \frac{2l+1}{z}\,j_l(z) \tag{16}$$

in the following section.

More information on the spherical Bessel functions can be found in the classical monograph by Watson [1] and in chapter 10 of the *Handbook of Mathematical Functions* [2].

2.3. *Derivation of the explicit formula*

Theorem 1. Let (l_1, l_2, l_3) be non-negative integers which can form the sides of a plane triangle and whose sum is an *even* integer. Let (p_1, p_2, p_3) be non-negative real numbers. Then the function $I_{l_1,l_2,l_3}(p_1, p_2, p_3)$ is given by

$$I_{l_1,l_2,l_3}(p_1,p_2,p_3) = \frac{4p_1p_2p_3}{\pi}\int_0^\infty x^2 j_{l_1}(p_1x)j_{l_2}(p_2x)j_{l_3}(p_3x)\,\mathrm{d}x \tag{17}$$

$$\begin{aligned}
&= \Delta(p_1,p_2,p_3)(-1)^{(l_1+l_2+l_3)/2}\frac{1}{2}\sum_{k_1=0}^{l_1}\sum_{k_2=0}^{l_2}\sum_{k_3=0}^{l_3}\frac{(-1)^{(k_1+k_2+k_3)}}{(k_1+k_2+k_3)!}\\
&\quad\times\frac{(l_1+k_1)!(l_2+k_2)!(l_3+k_3)!}{k_1!(l_1-k_1)!k_2!(l_2-k_2)!k_3!(l_3-k_3)!}(2p_1)^{-k_1}(2p_2)^{-k_2}(2p_3)^{-k_3}\\
&\quad\times[(-1)^{(l_1+k_1)}(p_2+p_3-p_1)^{(k_1+k_2+k_3)} + (-1)^{(l_2+k_2)}(p_3+p_1-p_2)^{(k_1+k_2+k_3)}\\
&\quad+(-1)^{(l_3+k_3)}(p_1+p_2-p_3)^{(k_1+k_2+k_3)} - (p_2+p_3+p_1)^{(k_1+k_2+k_3)}].
\end{aligned} \tag{18}$$

Thus the function vanishes unless the numbers p_1, p_2, p_3 can be the sides of a plane triangle.

Proof. Equation (14) shows that the integrand of (17) is an even function of x when $l_1+l_2+l_3$ is even; thus the integration can be extended to the whole real line and we have

$$I_{l_1,l_2,l_3}(p_1, p_2, p_3) = \frac{2p_1p_2p_3}{\pi}\int_{-\infty}^{+\infty} x^2 j_{l_1}(p_1x) j_{l_2}(p_2x) j_{l_3}(p_3x)\,\mathrm{d}x. \tag{19}$$

Consider first the case in which (p_1, p_2, p_3) do not form a plane triangle. It suffices to assume that $p_3 > p_1 + p_2$. Then by equations (11)–(13), we see that

$$I_{l_1,l_2,l_3}(p_1, p_2, p_3) = 2\,\mathrm{Re}\left\{\frac{p_1p_2p_3}{\pi}\mathcal{P}\int_{-\infty}^{+\infty} x^2 j_{l_1}(p_1x) j_{l_2}(p_2x) h^{(1)}_{l_3}(p_3x)\,\mathrm{d}x\right\} \tag{20}$$

where $\mathcal{P}$ denotes the Cauchy principal value. In fact the only singularity is a removable singularity at the origin; the integrand has leading power $x^{l_1+l_2-l_3+1}$ near $x = 0$, whose exponent is at least 1 because of the hypothesis that l_1, l_2, l_3 form a triangle. Now as a line integral in the z-plane, where $x = \mathrm{Re}\,z$, we may associate (20) with the contour integral around a D-shaped contour (figure 1) consisting of the line segment $[-R, +R]$ and a semicircle γ in the upper half-plane taken in the positive sense.

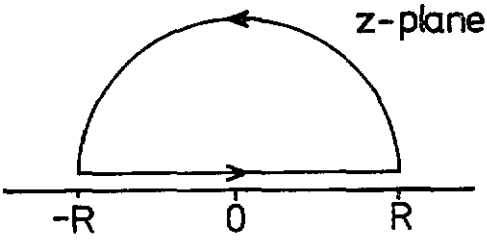

Figure 1. Contour for evaluation of (20).

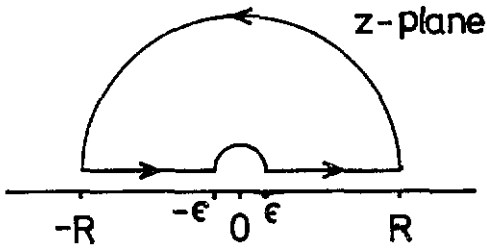

Figure 2. Contour for evaluation of (21).

Since the the integrand has, at most, a removable singularity at $z = 0$ and is holomorphic elsewhere in C its contour integral vanishes by Cauchy's theorem. It only remains to prove that the integral over the semicircular arc vanishes as $R \to \infty$ to be able to conclude that the right-hand side of (24) vanishes. This is straightforward if we consider equations (11)–(13), which show that on this arc,

$$|j_l(pz)| = \frac{\mathrm{e}^{p\,\mathrm{Im}\,z}}{pR}\left(1 + \mathrm{O}\left(\frac{1}{R}\right)\right) \qquad \mathrm{Im}\,z > 0.$$

Thus since, by hypothesis, $k = p_3 - p_1 - p_2$ is positive

$$\left|\frac{p_1p_2p_3}{\pi}\int_\gamma z^2 j_{l_1}(p_1z) j_{l_2}(p_2z) h^{(1)}_{l_3}(p_3z)\,\mathrm{d}z\right| \leqslant \int_0^\pi \mathrm{e}^{(p_1+p_2-p_3)R\sin\theta}\left(1 + \mathrm{O}\left(\frac{1}{R}\right)\right)\mathrm{d}\theta$$

$$\leqslant 2\int_0^{\pi/2} \mathrm{e}^{-2kR\theta/\pi}\left(1 + \mathrm{O}\left(\frac{1}{R}\right)\right)\mathrm{d}\theta = \frac{\pi}{kR}(1 - \mathrm{e}^{-kR})\left(1 + \mathrm{O}\left(\frac{1}{R}\right)\right)$$

where the second step has employed symmetry about $\theta = \pi/2$ and Jordan's inequality (for example [26] p 113). Thus the integral on γ vanishes, and so does $I_{l_1,l_2,l_3}(p_1, p_2, p_3)$.

Now consider the case when (p_1, p_2, p_3) can form a non-degenerate triangle. In this case we apply (13) to all the spherical Bessel functions in (1) so that

$$I_{l_1,l_2,l_3}(p_1, p_2, p_3) = \frac{p_1 p_2 p_3}{4\pi} \times \mathcal{P} \int_{-\infty}^{+\infty} \{h_{l_1}^{(1)}(p_1x)h_{l_2}^{(1)}(p_2x)h_{l_3}^{(1)}(p_3x) + h_{l_1}^{(2)}(p_1x)h_{l_2}^{(2)}(p_2x)h_{l_3}^{(2)}(p_3x) + h_{l_1}^{(1)}(p_1x)h_{l_2}^{(1)}(p_2x)h_{l_3}^{(2)}(p_3x) + h_{l_1}^{(2)}(p_1x)h_{l_2}^{(2)}(p_2x)h_{l_3}^{(1)}(p_3x) + h_{l_1}^{(1)}(p_1x)h_{l_2}^{(2)}(p_2x)h_{l_3}^{(1)}(p_3x) + h_{l_1}^{(2)}(p_1x)h_{l_2}^{(1)}(p_2x)h_{l_3}^{(2)}(p_3x) + h_{l_1}^{(2)}(p_1x)h_{l_2}^{(1)}(p_2x)h_{l_3}^{(1)}(p_3x) + h_{l_1}^{(1)}(p_1x)h_{l_2}^{(2)}(p_2x)h_{l_3}^{(2)}(p_3x)\}x^2\,dx. \quad (21)$$

The second terms in each line of (21) are the complex conjugates of the first terms so that we need consider only the latter. This time, we must use the contour of figure 2, which resembles that of figure 1, but has also a semicircular indentation σ of radius ϵ so that the contour passes above the multiple pole at the origin.

When (p_1, p_2, p_3) can form a triangle, the inequalities (6) show that $p_1 + p_2 + p_3$, $p_1 + p_2 - p_3$, $p_1 - p_2 + p_3$, $-p_1 + p_2 + p_3$ are all positive, so that an argument similar to that used when (p_1, p_2, p_3) do not form a triangle shows that the integrals all vanish as $R \to \infty$ on the semicircular arc γ. As before, the integrands are holomorphic within and on the contour, and so by applying Cauchy's theorem before passing to the limit as $\epsilon \to 0$, we arrive at the conclusion that $I_{l_1,l_2,l_3}(p_1, p_2, p_3)$ is equal to $(-i\pi)$ times the sum of the residues at $z = 0$. A tedious but straightforward calculation using equations (11), (12) leads directly to the required result.

Degenerate cases, for example $p_3 \to 0$ or $p_3 \to p_1 + p_2$, are best regarded as limiting cases of the general formula (18). □

The formula (18) is of limited usefulness. It neatly displays the symmetry of $I_{l_1,l_2,l_3}(p_1, p_2, p_3)$ with respect to permutation of the subscripts (1, 2, 3), and the fact that the function is rational, homogeneous and of degree zero. Moreover (p_1, p_2, p_3) must be able to form a plane triangle to get a non-zero result. If $\boldsymbol{p}_1$, $\boldsymbol{p}_2$ and $\boldsymbol{p}_3$ are 3-vectors with norms p_1, p_2 and p_3 then the triangle condition is equivalent to the statement $\boldsymbol{p}_1 + \boldsymbol{p}_2 + \boldsymbol{p}_3 = 0$; this therefore imposes conservation of 3-momentum at each vertex of a Feynman diagram.

The condition that $l_1 + l_2 + l_3$ be an even integer is necessary for the derivation of formula (18) but the condition that l_1, l_2, l_3 can form a triangle is only used to show that $I_{l_1,l_2,l_3}(p_1, p_2, p_3) = 0$ when $\Delta(p_1, p_2, p_3) = 0$. It is clear that the sum (18) has a meaning even when $\Delta(l_1, l_2, l_3) = 0$, but it is then no longer possible to conclude that $I_{l_1,l_2,l_3}(p_1, p_2, p_3)$ still vanishes when $\Delta(p_1, p_2, p_3) = 0$. This observation can sometimes be useful if we need to evaluate $I_{l_1,l_2,l_3}(p_1, p_2, p_3)$ from (18) to obtain starting values for the recursive algorithms of the next section.

The main disadvantage of (18) is its complexity. Whilst it is trivial to write $I_{l_1,l_2,l_3}(p_1, p_2, p_3)$ as a rational function of $\sin\theta_i$, the formula is very inconvenient for numerical calculation. Although the function is clearly well behaved in any limit $p_3 \to 0$ or $p_3 \to p_1 + p_2$, this involves a delicate cancellation of negative powers of p_i which is not easy to automate. This is largely avoided in the recursive method algorithms of the next section.

3. Recursive construction of $I_{l_1,l_2,l_3}(p_1, p_2, p_3)$

The numerical construction of the integrals $I_{l_1,l_2,l_3}(p_1, p_2, p_3)$ can best be accomplished by a recursive scheme, taking advantage of the fact that in the target application—the calculation of the self-energy of a bound atomic electron—at least one spherical Bessel function will have low order. Thus we can take one parameter, say l_1, to have the values 0, 1 or 2 in the first instance. The algorithm required depends on a family of auxiliary integrals which we shall discuss first.

3.1. The auxiliary integrals $H_{l_2}^{l_1}(\theta_1, \theta_2, \theta_3)$

A class of integrals related to the discontinuous integrals of Weber and Schafheitlin is treated by Watson [1], section 13.46; see also Gradshteyn and Ryzhik [3], formula 6.578.8. Let the non-negative reals a, b, c satisfy $\Delta(a, b, c) = 1$ and let A, B, C be the angles opposite to the sides of length a, b, c in a plane triangle. Then ([1], section 13.46)

$$\int_0^\infty J_\mu(at)J_\nu(bt)J_\nu(ct)t^{1-\mu}\,\mathrm{d}t = \frac{(bc)^{\mu-1}\sin^{\mu-1/2}A}{(2\pi)^{1/2}a^\mu}P_{\nu-1/2}^{1/2-\mu}(\cos A) \tag{22}$$

where $P_\alpha^\beta(x)$ is an associated Legendre function of the first kind, $\mathrm{Re}(\mu) > -\frac{1}{2}$ and $\mathrm{Re}(\nu) > -\frac{1}{2}$. The integral vanishes if $\Delta(a, b, c) = 0$. Putting $\mu = l_1 + \frac{1}{2}$, $\nu = l_2 + \frac{1}{2}$, $a = p_1$, $b = p_2$, $c = p_3$, $A = \theta_1$, $B = \theta_2$, $C = \theta_3$, we can define a new function

$$\begin{aligned} H_{l_2}^{l_1}(\theta_1, \theta_2, \theta_3) &:= \frac{4p_1p_2p_3}{\pi}\int_0^\infty x^2(p_1x)^{-l_1}j_{l_1}(p_1x)j_{l_2}(p_2x)j_{l_2}(p_3x)\,\mathrm{d}x \\ &= (2\pi p_1p_2p_3)^{1/2}p_1^{-l_1}\int_0^\infty J_{l_1+1/2}(p_1x)J_{l_2+1/2}(p_2x)J_{l_2+1/2}(p_3x)x^{1/2-l_1}\,\mathrm{d}x \\ &= \left(\frac{\sin\theta_2\sin\theta_3}{\sin\theta_1}\right)^{l_1}P_{l_2}^{-l_1}(\cos\theta_1) \end{aligned} \tag{23}$$

where $l_2 \geqslant l_1$. Because of the recurrence relation ([2], formula 8.5.3)

$$(\nu - \mu + 1)P_{\nu+1}^\mu(\cos\theta) = (2\nu + 1)\cos\theta\,P_\nu^\mu(\cos\theta) - (\nu + \mu)P_{\nu-1}^\mu(\cos\theta) \tag{24}$$

valid for $\nu = -\mu, -\mu + 1, \ldots$, and the formula

$$P_l^{-l}(\cos\theta) = (\sin^l\theta)/2^l l! \tag{25}$$

the functions

$$G_\nu^l(\theta) := 2^l l!(\sin\theta)^{-l}P_\nu^{-l}(\cos\theta) \tag{26}$$

with $\nu \geqslant l$, are polynomials in $\cos\theta$ so that we can write

$$H_{l_2}^{l_1}(\theta_1, \theta_2, \theta_3) = F_{l_1}(\theta_2, \theta_3)G_{l_2}^{l_1}(\theta_1) \tag{27}$$

where

$$F_l(\theta_2, \theta_3) := (\sin^l\theta_2\sin^l\theta_3)/(2^l l!). \tag{28}$$

It follows that $H_{l_2}^{l_1}(\theta_1, \theta_2, \theta_3)$ is a trigonometric polynomial function of its arguments. It can be generated directly by the following algorithm:

Algorithm 1. Evaluate (28) with $G_l^l = 1.0$ and

$$a_l^k = (l-k)/(l+k+1) \tag{29}$$

then

$$G_{k+1}^l(\theta_1) = \cos\theta_1(1-a_l^k)G_k^l(\theta_1) + a_l^k G_{k-1}^l(\theta_1) \tag{30}$$

for $k = l, l+1, l+2, \ldots$, from which $H_{l_2}^{l_1}(\theta_1, \theta_2, \theta_3)$ can be constructed using (27).

It is clear that this linear recurrence relation is stable as k increases.

3.2. Algorithms for the generation of $I_{l_1,l_2,l_3}(p_1, p_2, p_3)$

It is convenient to generate the integrals in successive 'layers' characterized by the value of l_1.

3.2.1. The layer $l_1 = 0$.

Algorithm 2.

$$I_{0,l,l}(p_1, p_2, p_3) = H_l^0(\theta_1, \theta_2, \theta_3) = P_l(\cos\theta_1). \tag{31}$$

From the symmetry of the function $I_{l_1,l_2,l_3}(p_1, p_2, p_3)$ with respect to its arguments, it follows immediately that

$$I_{l,0,l}(p_1, p_2, p_3) = P_l(\cos\theta_2) \tag{32}$$

$$I_{l,l,0}(p_1, p_2, p_3) = P_l(\cos\theta_3). \tag{33}$$

3.2.2. The layer $l_1 = 1$. In this case, we begin by applying (20) in the form

$$j_l(z) = \frac{z}{2l+1}[j_{l-1}(z) + j_{l+1}(z)] \tag{34}$$

to the last spherical Bessel function in the equation

$$H_l^1(\theta_1, \theta_2, \theta_3) = \frac{4p_1p_2p_3}{\pi}\int_0^\infty x^2(p_1x)^{-1}j_1(p_1x)j_l(p_2x)j_l(p_3x)\,dx$$

yielding the formula

$$H_l^1(\theta_1, \theta_2, \theta_3) = \frac{\sin\theta_3}{(2l+1)\sin\theta_1}\{I_{1,l,l+1}(p_1, p_2, p_3) + I_{1,l,l-1}(p_1, p_2, p_3)\}. \tag{35}$$

Similarly, applying (16) to the second spherical Bessel function gives

$$H_l^1(\theta_1, \theta_2, \theta_3) = \frac{\sin\theta_2}{(2l+1)\sin\theta_1}\{I_{1,l+1,l}(p_1, p_2, p_3) + I_{1,l-1,l}(p_1, p_2, p_3)\}. \tag{36}$$

The selection rules on the indices l_1, l_2, l_3 imply that that all the non-zero functions in the layer can be generated recursively from these two relations if we know the functions $I_{1,0,1}(p_1, p_2, p_3)$ and $I_{1,1,0}(p_1, p_2, p_3)$ (figure 3).

Algorithm 3. Initialize the non-zero elements on lines $l_2 = 1$ and $l_3 = 1$:

$$I_{1,1,0}(p_1, p_2, p_3) = P_1(\cos\theta_3) \qquad I_{1,0,1}(p_1, p_2, p_3) = P_1(\cos\theta_2). \tag{37}$$

Then for each $l = 1, 2, \ldots$,

$$I_{1,l,l+1}(p_1, p_2, p_3) = \frac{(2l+1)\sin\theta_1}{\sin\theta_3}H_l^1(\theta_1, \theta_2, \theta_3) - I_{1,l,l-1}(p_1, p_2, p_3) \tag{38}$$

$$I_{1,l+1,l}(p_1, p_2, p_3) = \frac{(2l+1)\sin\theta_1}{\sin\theta_2}H_l^1(\theta_1, \theta_2, \theta_3) - I_{1,l-1,l}(p_1, p_2, p_3). \tag{39}$$

The functions $H_l^1(\theta_1, \theta_2, \theta_3)$ are generated using algorithm 1.

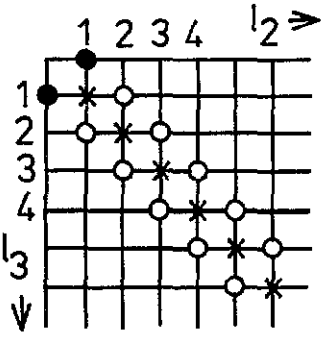

Figure 3. Construction of the layer $l_1 = 1$: ●, initial values from layer $l_1 = 0$; ×, values of H_l^1; ○, computed values.

3.2.3. The layer $l_1 = 2$. Two applications of (34) are required in order to generate the recurrence relations in this layer. For reasons of legibility, here we drop the arguments θ_i, provided we remember that it is no longer permissible to permute the indices l_i. We must reinstate the θ_i if it is necessary to do this. Applying (34) twice to the third and the second spherical Bessel functions defining $H_{l_2}^{l_1}$ in (23) gives, respectively,

$$H_l^2 = \frac{\sin^2\theta_3}{\sin^2\theta_1}\left[\frac{I_{2,l,l-2}}{(2l-1)(2l+1)} + \frac{2I_{2,l,l}}{(2l-1)(2l+3)} + \frac{I_{2,l,l+2}}{(2l+1)(2l+3)}\right] \tag{40}$$

and

$$H_l^2 = \frac{\sin^2\theta_2}{\sin^2\theta_1}\left[\frac{I_{2,l-2,l}}{(2l-1)(2l+1)} + \frac{2I_{2,l,l}}{(2l-1)(2l+3)} + \frac{I_{2,l+2,l}}{(2l+1)(2l+3)}\right]. \tag{41}$$

A third recurrence relation appears if we use (34) once each on the second and third spherical Bessel functions, giving

$$H_l^2 = \frac{\sin\theta_2\sin\theta_3}{(2l+1)^2\sin^2\theta_1}[I_{2,l-1,l-1} + I_{2,l+1,l-1} + I_{2,l-1,l+1} + I_{2,l+1,l+1}]. \tag{42}$$

The three recurrence relations generate patterns connecting points on the (l_2, l_3) lattice covering the $l_1 = 2$ layer as shown in figure 4.

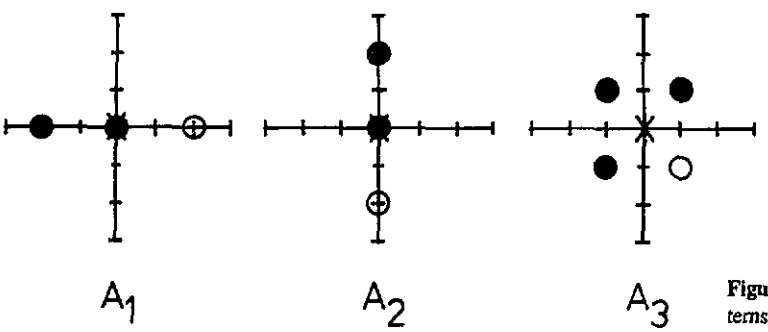

Figure 4. Recurrence patterns in the layer $l_1 = 2$.

Examining the pattern of figure 5, we see that we need an additional starting value, $I_{2,2,2}$, which cannot be obtained from lower layers. This quantity can be constructed from

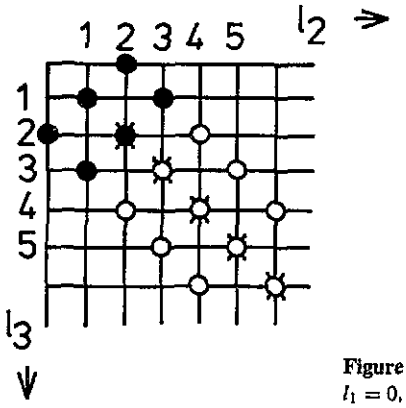

Figure 5. Construction of the layer $l_1 = 2$: ●, initial values from layers $l_1 = 0, 1$; ×, values of H_l^2; ○, computed values.

(22), rewritten in terms of the angles $\theta_1, \theta_2, \theta_3$, a tedious operation for which we have used the MAPLE V, version 2 system. The result is

$$I_{2,2,2}(p_1, p_2, p_3) = \frac{1}{8} + \frac{3}{8}\left\{\frac{\sin^2\theta_1 \cos\theta_1}{\sin\theta_2 \sin\theta_3} + \frac{\sin^2\theta_2 \cos\theta_2}{\sin\theta_3 \sin\theta_1} + \frac{\sin^2\theta_3 \cos\theta_3}{\sin\theta_1 \sin\theta_2}\right\}. \tag{43}$$

Algorithm 4. First initialize the non-zero values $I_{2,2,0}$, $I_{2,0,2}$ on the lines $l_3 = 0$ and $l_2 = 0$ respectively; $I_{2,1,1}$, $I_{2,3,1}$ and $I_{2,1,3}$ on the lines $l_3 = 1$ and $l_2 = 1$ respectively using the relevant entries from layers 0, 1; and $I_{2,2,2}$ from (43).

Then for $l = 2, 3, \ldots$ calculate successively

$$I_{2,l,l+2} = (2l+1)(2l+3)\frac{\sin^2\theta_1}{\sin^2\theta_3}H_l^2 - \frac{2(2l+1)}{(2l-1)}I_{2,l,l} - \frac{(2l+3)}{(2l-1)}I_{2,l,l-2} \tag{44}$$

corresponding to pattern A_1 of figure 4; and

$$I_{2,l+2,l} = (2l+1)(2l+3)\frac{\sin^2\theta_1}{\sin^2\theta_2}H_l^2 - \frac{2(2l+1)}{(2l-1)}I_{2,l,l} - \frac{(2l+3)}{(2l-1)}I_{2,l-2,l} \tag{45}$$

corresponding to pattern A_2; and

$$I_{2,l+1,l+1} = (2l+1)^2\frac{\sin^2\theta_1}{\sin\theta_2 \sin\theta_3}H_l^2 - I_{2,l-1,l-1} - I_{2,l+1,l-1} - I_{2,l-1,l+1} \tag{46}$$

corresponding to pattern A_3 of figure 4.

3.2.4. Layers with $l_1 \geqslant 3$. The major uses of the algorithms so far described only require layers $l_1 = 0, 1, 2$, with l_2, l_3 taking values up to about 40 or 50. However, for completeness, we now describe the procedure for higher layers whose structure is easy to understand when one examines what we have done so far.

(i) Initialize on the lines $l_2 = k$, $l_3 = k$, $k = 0, 1, \ldots, m-1$. This is accomplished by using results from layers $l_1 = 0, 1, \ldots, m-1$ in combination with the symmetry relation (7). Missing values on lines $l_2 + l_3 = 2m$ if m is even or $l_2 + l_3 = 2m + 1$ if m is odd may be obtained from (18).

(ii) Next calculate the integrals H_l^m, $l \geqslant m$ using algorithm 1.

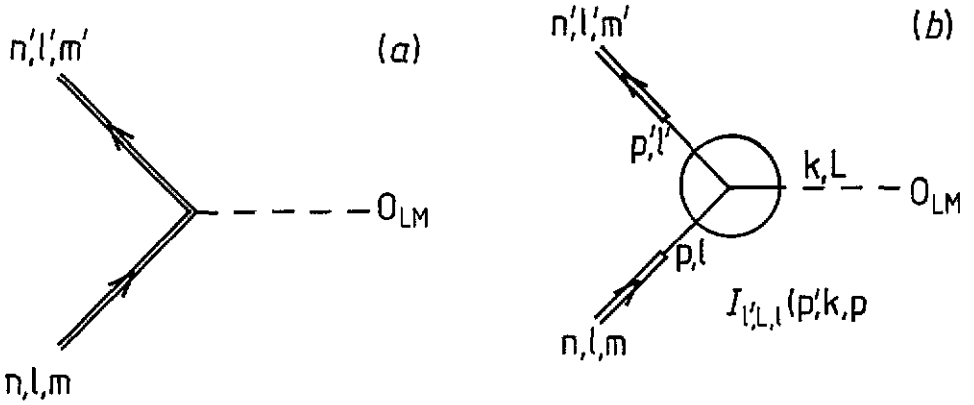

Figure 6. (*a*) Diagrammatic representation of (51). The double lines represent bound states; the dashed line represents the multipole operator. (*b*) Expansion of the one-electron matrix element in terms of free particle spherical waves.

(iii) The remaining entries in layer m can be computed using the $m+1$ recurrence relations $A_1, A_2, \ldots, A_{m+1}$ which generalize the three relations A_1, A_2, A_3 of algorithm 4. These are applied in succession to generate the integrals with $l_2 \geqslant m$, $l_3 \geqslant m$, starting on the diagonal with $I_{m,m,m}$ when m is even or on the immediately adjacent sub- and super-diagonal lines with $I_{m,m,m+1}$ and $I_{m,m+1,m}$ when m is odd, and working outwards to the limits set by the selection rules. Thus on the line l_3, the non-zero entries satisfy $l_3 = |l_1 - l_2|, \ldots, l_1 + l_2$ with $l_1 + l_2 + l_3$ an even integer. This makes alternate entries vanish along the line.

4. Some applications

A simple problem which brings out some of the consequences of the selection rules on linear and angular momentum permits verification of the algorithms described in the last section. We consider first a simple process in which a (non-relativistic) bound electron in a state described by quantum numbers n, l interacts with a multipole field proportional to $O_{L,M} = j_L(kr)Y_L^M(\theta, \phi)$ and enters a state with quantum numbers n', l'. The matrix element is

$$\langle n', l', m'|O_{L,M}|n, l, m\rangle \tag{47}$$

which can be represented by the diagram in figure 6(*a*). This expression can be evaluated in a straightforward manner; the angular momentum selection rules require that

$$|l - l'| \leqslant L \leqslant l + l' \qquad l' + L + l \text{ an even integer} \tag{48}$$

Standard results of angular momentum theory (for example in [27]) enable us to write this in the form

$$\langle n', l', m'|O_{L,M}|n, l, m\rangle = (-1)^{l'-m'}\left(\frac{[l', L, l]}{4\pi}\right)^{1/2}\begin{pmatrix} l' & L & l \\ 0 & 0 & 0\end{pmatrix}\begin{pmatrix} l' & L & l \\ -m' & M & m\end{pmatrix}T^L_{n'l',nl} \tag{49}$$

where $[l', L, l] = (2l' + 1)(2L + 1)(2l + 1)$ and

$$T^L_{n'l',nl}(k)\int_0^\infty R^*_{n'l'}(r)j_L(kr)R_{nl}(r)r^2\,\mathrm{d}r. \tag{50}$$

The angular momentum selection rules are implicit in the $3j$ symbols appearing in this expression.

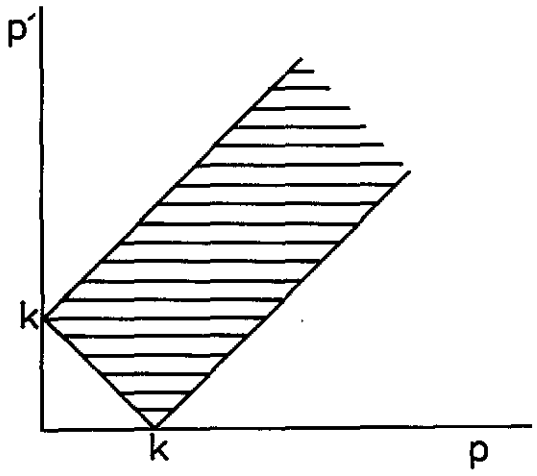

Figure 7. The region of integration in equation (56).

Now let us suppose that the radial amplitudes $R_{nl}(r)$ possess (spherical) Hankel transforms. The functions $R_{nl}(r)$ and $S_{nl}(k)$ are said to be (spherical) Hankel transform pairs [28, 29] if

$$R_{nl}(r) = \sqrt{\frac{2}{\pi}} \int_0^\infty S_{nl}(k) j_l(kr) k^2 \, \mathrm{d}k \tag{51}$$

$$S_{nl}(k) = \sqrt{\frac{2}{\pi}} \int_0^\infty R_{nl}(r) j_l(kr) r^2 \, \mathrm{d}r. \tag{52}$$

These relations are equivalent to the statements

$$\int_0^\infty j_l(kr) j_l(kr') k^2 \, \mathrm{d}k = \frac{\pi}{2r^2} \delta(r - r') \tag{53}$$

$$\int_0^\infty j_l(kr) j_l(k'r) r^2 \, \mathrm{d}r = \frac{\pi}{2k^2} \delta(k - k'). \tag{54}$$

Inserting (51) in (49) and using (1), we see that

$$T^L_{n'l',nl}(k) = \frac{1}{2k} \int \int S^*_{n'l'}(p') I_{l',L,l}(p', k, p) S_{nl}(p) p' \mathrm{d}p' p \, \mathrm{d}p. \tag{55}$$

We can represent this in terms of the diagram in figure 6(*b*).

Since $I_{l',L,l}(p', k, p)$ vanishes unless p', k, p can form the sides of a plane triangle, the domain of integration over p', p is restricted to the region shown in figure 7. This has the effect that

$$\lim_{k \to 0} \frac{1}{2k} I_{l,0,l}(p', k, p) = \delta(p' - p) \delta_{l,0} \tag{56}$$

which highlights the meaning of the integral $I_{l',L,l}(p', k, p)$ as a distribution. For a demonstration, suppose that $0 < k < p, 0 < k < p'$, and consider

$$\int_{p-k}^{p+k} f(p', k, p) \, \frac{1}{2k} I_{l,0,l}(p', k, p) \, \mathrm{d}p'$$

where $f(p', k, p)$ is a continuous and integrable function. Putting $p' = p + tk$, $-1 < t < 1$, we see that this becomes

$$\frac{1}{2} \int_{-1}^{1} f(p + tk, k, p) I_{l,0,l}(p + tk, k, p) \, \mathrm{d}t$$

which reduces with the aid of (32) to $f(p,0,p)P_l(1)$ from which (56) follows immediately. It follows that

$$\int_0^\infty R^*_{n'l}(r)R_{nl}(r)r^2\,\mathrm{d}r = \int_0^\infty S^*_{n'l}(p')S_{nl}(p)p^2\,\mathrm{d}p \tag{57}$$

as expected.

The renormalization algorithm of [11] requires the evaluation of

$$\begin{aligned} M_0 = \frac{\alpha}{\pi}mc^2 \sum_{\nu,\lambda}\sum_{\kappa,m,a}\int_0^\infty \mathrm{d}p' \int_0^\infty k\,\mathrm{d}k \sum_{\mu,\mu'=0}^{3} g_{\mu\mu'} \\ \times \int_{|p-k|}^{p+k} \mathrm{d}p_1\, \hat{\Psi}_0^\dagger(p_1,+1)\Omega^\mu(p_1,+1,\kappa_0,m_0;k,\nu,\lambda;p,a,\kappa,m) \\ \times \int_{|p-k|}^{p+k} \mathrm{d}p_2 \frac{\Omega^{\mu'}(p_2,+1,\kappa_0,m_0;k,\nu,\lambda;p,a,\kappa,m)^\dagger}{E(p,a)-E(p_2,+1)-ack}\hat{\Psi}_0(p_2,+1) \end{aligned} \tag{58}$$

where $g_{\mu,\mu'}$ is the usual Minkowski metric, $\{+1,-1,-1,-1\}$,

$$E(p,a) = ac\sqrt{p^2+m^2c^2}$$

is the energy of a free electron and

$$a := \operatorname{sgn} E(p,a)$$

which takes the value $+1$ for electron states and -1 for positron (negative energy) states. The momentum wavefunction of the state whose self-energy is being calculated is denoted by $\hat{\Psi}_0(p,+1)$, a solution of Dirac's equation in a local mean field potential, and

$$\begin{aligned} &\langle\Psi_0|\,\alpha^\mu C^\nu_\lambda(\theta,\phi)j_\nu(kr)\,|\,p',\kappa',a'\rangle \\ &\quad = \int_{|p-k|}^{p+k}\mathrm{d}p_1\,\hat{\Psi}_0^\dagger(p_1,+1)\Omega^\mu(p_1,+1,\kappa_0,m_0;k,\nu,\lambda;p,a,\kappa,m) \end{aligned} \tag{59}$$

is a radiative transition matrix element from the bound state into a free electron virtual state [30]. Here we have used (51) to express the bound state as a linear combination of free electron states of the form

$$\Psi_{p,\kappa,m}(\mathbf{r}) = \frac{1}{r}\begin{bmatrix} \left(\frac{E+mc^2}{\pi E}\right)^{1/2} & \rho j_l(\rho) & \chi_{\kappa,m}(\theta,\phi) \\ \mathrm{i}\left(\frac{E-mc^2}{\pi E}\right)^{1/2} & \rho j_{\bar{l}}(\rho) & \chi_{-\kappa,m}(\theta,\phi) \end{bmatrix} \tag{60}$$

in spherical polar coordinates. Here $\rho = pr$; κ is related to the total angular momentum of the state by $\kappa = \pm(j+\frac{1}{2})$, $j = \frac{1}{2},\frac{3}{2},\ldots$; $l = \kappa, \bar{l} = \kappa - 1$ if $\kappa > 0$ and $l = -\kappa - 1, \bar{l} = -\kappa$ if $\kappa < 0$; and $\chi_{\kappa,m}(\theta,\phi)$ is a spin–orbit eigenfunction [31]. With this normalization the states (60) are normalized to a delta function of energy $E(p,a)$. Also α^μ is a 4×4 Dirac matrix, and $C^\nu_\lambda(\theta,\phi)$ is a spherical harmonic, standardized in the manner of [27].

After carrying out the angular integrations, the matrix elements (59) can be written [30, 31] as linear combinations of integrals over Dirac radial components of the form

$$\begin{aligned} I^\pm_L &= \int_0^\infty [\overline{P(r)}Q'(r) \pm \overline{Q(r)}P'(r)]j_L(kr)\mathrm{d}r \\ J_L &= \int_0^\infty [\overline{P(r)}P'(r) + \overline{Q(r)}Q'(r)]j_L(kr)\mathrm{d}r. \end{aligned}$$

where $P(r)$ is an upper component and $Q(r)$ is a lower component and the bars denote complex conjugation. After taking account of the transform (51), we see that these integrals are linear combinations of the vertex integrals $I_{l,L,l'}(p, k, p')$. In the renormalization problem for s- and $p_{1/2}$-states, only vertex integrals with $l = 0, 1$ appear, though the multipole order L, and therefore l', may be as high as 30–50. The triangle conditions on the momentum arguments in (59) mean that the innermost quadratures over p_1 and p_2 are confined to the finite interval $(|p - k|, p + k)$, so that there are only two integrations over an infinite range. It is possible to show that these integrals are finite, so that M_0 is a sum of finite contributions. The sum over ν is logarithmically divergent, as expected. However, if individual terms of (59) are subtracted from the corresponding terms in which the virtual electron propagates in the atomic field, the resulting sum over ν converges to the observable self-energy shift [11]. No other regularization is needed.

5. Discussion

We have devised a new recursive algorithm for the vertex integrals $I_{l',L,l}(p', k, p)$ which is particularly well suited to production in the large numbers required for computing the electron self-energy in atomic structure [11]. The algorithm is both fast and accurate, capable of calculating the integrals to machine precision. For s- and $p_{1/2}$-state renormalization, the four-dimensional integration requires some 10^4–10^5 vertex integrals in each run. It is possible to code the algorithms for efficient evaluation on vector processors. The complete self-energy calculation runs in a few tens of minutes on a Sun SPARCstation ELC.

Other algorithms, for example, the evaluation of the explicit formula (18) or the equivalent Jackson–Maximon formula [7], are less attractive for this type of calculation. The latter requires the evaluation of the tensor product of rank 0 of three spherical harmonics

$$\sum_{m_1,m_2,m_3} \begin{pmatrix} l_1 & l_2 & l_3 \\ m_1 & m_2 & m_3 \end{pmatrix} Y_{l_1}^{m_1}(\theta_1, \phi_1) Y_{l_2}^{m_2}(\theta_2, \phi_2) Y_{l_3}^{m_3}(\theta_3, \phi_3).$$

Jackson and Maximon propose a recursive algorithm for evaluating each such sum which has a much more complicated structure than our procedure and which seems in principle less well suited to mass calculation of vertex integrals. Like our own formula (18) it is impossible to avoid cancellations with attendant numerical inaccuracies.

Acknowledgments

We should like to thank Dr Tony Scott for his help in verifying many of the results of this paper using MAPLE. We are indebted to Dr Radoslaw Szmytkowski of the University of Gdansk for drawing our attention to references [9, 10] and to an anonymous referee for drawing our attention to reference [7].

References

[1] Watson G N 1958 *A Treatise on the Theory of Bessel Functions* 2nd edn (Cambridge: Cambridge University Press) pp 411–2

[2] Abramowitz M and Stegun I A (eds) 1970 *Handbook of Mathematical Fuctions* (New York: Dover) p 487

[3] Gradshteyn I S and Ryzhik I M 1965 *Table of Integrals Series and Products* transl. by A Jeffrey (New York: Academic Press) p 694
[4] Bailey W N 1935 *Proc. Lond. Math. Soc.* **40** 37
[5] Gervois A and Navelet H 1984 *J. Math. Phys.* **25** 3350–6
[6] Gervois A and Navelet H 1989 *SIAM J. Math. Anal.* **20** 1006–8
[7] Jackson A D and Maximon L C 1972 *SIAM J. Math. Anal.* **3** 446–60
[8] Danos M, Stahlhofen A A and Biedenharn L C 1989 *Ann. Phys., NY* **192** 158–205
[9] Davies K T R and Davies R W 1989 *Can. J. Phys.* **67** 759
[10] Davies K T R, Strayer M R and White G D 1988 *J. Phys. G: Nucl. Phys.* **14** 961
[11] Quiney H M and Grant I P 1993 *Phys. Scr.* T **46** 132–8
[12] Feynman R P 1948 *Phys. Rev.* **74** 1430
[13] Feynman R P 1949 *Phys. Rev.* **76** 769
[14] Series G W 1988 *The Spectrum of Atomic Hydrogen: Advances* (Singapore: World Scientific)
[15] Brown G E, Langer J S and Schaefer G W 1959 *Proc. R. Soc.* A **251** pp 92–104
[16] Brown G E and Mayers D F 1959 *Proc. R. Soc.* A**251** pp 105–109
[17] Desiderio A M and Johnson W R 1971 *Phys. Rev.* A **3** 1267
[18] Mohr P J 1974 *Ann. Phys., NY* **88** 26, 52
[19] Mohr P J 1982 *Phys. Rev.* A **26** 2338
[20] Johnson W R and Soff G 1985 *Atom. Data Nucl. Data Tables* **33** 405
[21] Mohr P J and Kim Y K 1992 *Phys. Rev.* A **45** 2727
[22] Cheng K T and Johnson W R 1976 *Phys. Rev.* A **14** 1943
[23] Cheng K T, Johnson W R and Snyderman N J *Phys. Rev. Lett.* **66** 2960
[24] Snyderman N J *Ann. Phys., NY* **211** 43
[25] Blundell S A and Snyderman N J 1991 *Phys. Rev.* A **44** R1427
[26] Priestley H A 1990 *Introduction to Complex Analysis* revised edn (Oxford: Clarendon)
[27] Brink D M and Satchler G R 1968 *Angular Momentum* 2nd edn (Oxford: Clarendon)
[28] Titchmarsh E C 1948 *Introduction to the theory of Fourier Integrals* 2nd edn, section 8.18 (Oxford: Clarendon)
[29] Erdelyi A, Magnus W, Oberhettinger F and Tricomi F G 1952 *Tables of Integral Transforms* vol 2, ch VIII (New York: McGraw-Hill)
[30] Grant I P 1974 *J. Phys. B: At. Mol. Phys.* **7** 1458
[31] Grant I P 1988 *Methods in Computational Chemistry* vol 2, ed S Wilson (New York: Plenum) pp 1–71